Port Said Engineering Research Journal
Faculty of Engineering – Port Said University
Volume 19 No. 2 September2015 pp: 76 : 86

A Comparative Performance Analysis and Flicker Assessment of SCIG and DFIG-Based Wind Turbines

Ali H. Kasem Alaboudy[1], Ahmed M. Azmy[2], and Walid S.E. Abdellatif[1]

ABSTRACT

This paper presents a comparative performance analysis of squirrel cage induction generator (SCIG) and doubly fed induction generator (DFIG) systems driven by wind turbines under different operating conditions. Also, the constant and variable-speed configurations are compared regarding short-term flicker severity, P_{st}. The constant speed configurations are based on SCIG in addition to SCIG equipped with static synchronous compensator (STATCOM) with the same generation capacity. In this paper, comprehensive models of wind turbine are used to analyze power and voltage fluctuations. The short-time flicker index is used to assess the emitted voltage fluctuation. The effects of grid short circuit capacity and impedance angle on flicker emission are investigated. The influences of site mean-wind-speed and turbulence intensity on voltage fluctuation are also examined. A flickermeter model is implemented according to the guidelines provided by IEC 61000-4-15 to evaluate the severity of voltage fluctuation emission. The models of different system components along with their control schemes are simulated using Matlab/Simulink® package.

Keywords— wind turbine, SCIG, DFIG, maximum power point tracking (MPPT), voltage flicker.

1. INTRODUCTION

The growing demand for electric energy all over the world has highly motivated the use of renewable sources of energy. Among renewable-based energy sources that have been intensively studied, wind energy seems to have a vital role in the near future. Over the last ten years, the global wind energy capacity has increased rapidly and became the fastest developing renewable energy technology [1]. Clean operation and minimal running cost requirements are some motivations of using more wind energy within power grids [2].

Most of the wind turbines use induction generators because of their advantageously characteristics; such as the over speed capability; make them suitable for integration with wind turbines; especially that are used squirrel cage induction generators (SCIG) because of its mechanical simplicity, high efficiency and low maintenance requirements, but at the present time doubly fed induction generator (DFIG) are widely used for large wind power plants [3].

The SCIG speed changes by only a few percent because of the generator slip caused by changes in wind speed. Therefore, this generator is often called the constant-speed wind generating system. Owing to the characteristics of constant-speed wind turbines, the active and reactive power exchange at the point of common coupling (PCC) is varying according to the wind speed fluctuations. As a result, the voltage at this point will also fluctuate. One of the possible solutions to overcome voltage flicker emission for constant speed wind turbines is to incorporate static synchronous compensator (STATCOM) [4].

During the last decades, DFIG-based wind turbines have been considered as the most preferred option for high-capacity wind farms because they have the ability to control the active and reactive power exchange within the network. DFIG have the capability to operate in variable speed modes and hence, a smooth operation can be achieved and the power can be doubled compared to other conventional generators [5]. Variable-speed wind turbines based on DFIG have shown better performance in comparison to constant-speed wind turbines based on SCIG. The reason is that variable-speed operation, controllable power factor, and improved system efficiency [6].

One of the most important wind power quality considerations is the effect of voltage fluctuations, voltage dips and harmonics mitigation. Which disturb the sensitive electric and electronic equipments. This may lead to a great reduction in the life span of most equipment. Flickers have widely been considered as a serious drawback and may limit the maximum amount of wind power generation that can be connected to the grid [7]. There are numerous factors that affect flicker emission of grid-connected wind turbines during continuous operation, such as wind characteristics (e.g. mean wind speed and turbulence intensity) and grid conditions (e.g. short circuit capacity, grid impedance angle and load type) [8]. The lighting flicker level is generally used to measure voltage fluctuation. Voltage fluctuation disturbs the sensitive electric and electronic equipment. And, hence, IEC 61400-21 is developed to provide procedures for determining the power quality characteristics of wind turbines especially flicker emissions [9].

In this paper, detailed models of constant-speed SCIG-based wind turbines and variable speed DFIG-based wind turbines are developed. This includes the control process and the standard flickermeter according to IEC 61000-4-15 to accurately evaluate the flicker emissions under different operating conditions. The

[1]Electrical Power, and Machines Department, Faculty of Industrial Education, Suez University, Suez, Egypt, E-mail: ali.alaboudy@suezuniv.edu.eg, walid.abdellatif@suezuniv.edu.eg

[2]Department of Electrical Engineering Faculty of Engineering, Tanta University, Tanta, Egypt, E-mail: azmy@f-eng.tanta.edu.eg.

SCIG is connected directly to the grid and the DFIG is connected to the grid at PCC via an ac-dc-ac back-to-back converter set. Two control schemes are developed for rotor-and grid-side converters. The control of the rotor-side converter is developed to apply maximum power point tracking (MPPT) strategy, while the control scheme of the grid-side converter is designed to operate at unity power factor and stabilize the dc link voltage to its nominal value. The analysis studies the effect of site parameters, i.e. mean wind speed and turbulence intensity, and grid parameters, i.e. grid short circuit ratio and grid impedance angle, on voltage fluctuations. Comprehensive models of the wind energy conversion system (WECS) and flickermeter considering system dynamics, and control actions are simulated using Matlab/Simulink® package.

2. SYSTEM MODELING

Wind energy conversion system converts wind kinetic energy to mechanical energy by means of wind turbine rotor blades. Then, the generator converts the mechanical power to electrical power that is being fed to the grid through power electronic converters. Fig.1 shows a simple layout of a 9 MW wind farm is simulated by three pairs of 1.5 MW wind turbines based on induction generators. A model for the system under study is implemented in Matlab/Simulink environment.
The WECS under study consists of two main parts:

a) Mechanical parts: include the aerodynamic system with the rotor blades and the gearbox.
b) Electrical parts: comprised of the induction generator (SCIG–DFIG) and the back-to-back converter set for DFIG system [10].

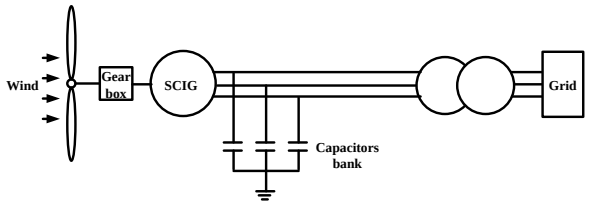

(a)

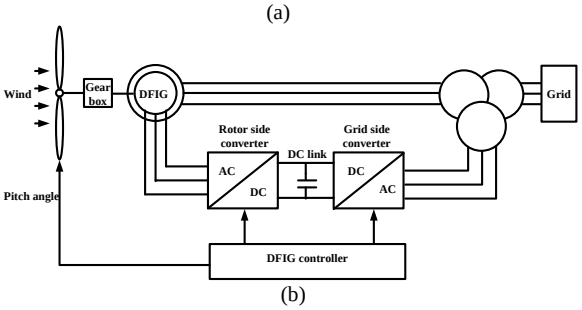

(b)

Fig. 1 (a) Constant speed SCIG directly grid connected wind turbines (b) Variable speed DFIG based wind turbine configuration [10].

2.1 Mechanical Parts of Wind Turbine System

It is well known that the aerodynamic rotor is responsible for converting available wind power to mechanical power through the wind turbine at the shaft.

The aerodynamic power of a wind turbine is given by the following equation [11]:

$$P_{aer} = \frac{1}{2}\rho\pi R^2 V^3 C_p(\lambda,\beta) \qquad (1)$$

where: ρ is the air density (kg/m^3), R is radius of the turbine blade (m), V is the wind speed (m/s), C_p is the power coefficient, λ the tip speed ratio and β is the blade pitch angle.

On the other hand, the tip-speed ratio is defined as:

$$\lambda = \frac{\omega_t R}{V} \qquad (2)$$

where: ω_t is the turbine angular speed.

From (1), to extract maximum available power at the available wind speed, V, the wind generator has to run at a particular speed that corresponds to wind speed in such a way that the maximum power point is tracked as shown in Fig.2. The objective of operating in the maximum power point tracking (MPPT) mode is to maximize power extraction at low to medium wind speeds.

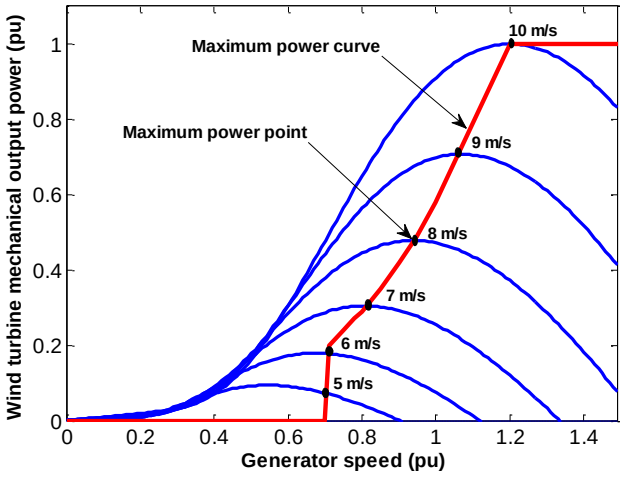

Fig.2. Wind turbine mechanical power output rotor speed [12].

2.2 Electrical Parts of Wind Turbine System

2.2.1 Induction machine modelling

Due to the speed flexibility of asynchronous machines, they are widely used in wind generation installations. The d-q equivalent circuit diagram of an induction machine is shown in Fig. 3. The electrical equations of the induction machine based on the equivalent circuit are found in [13].

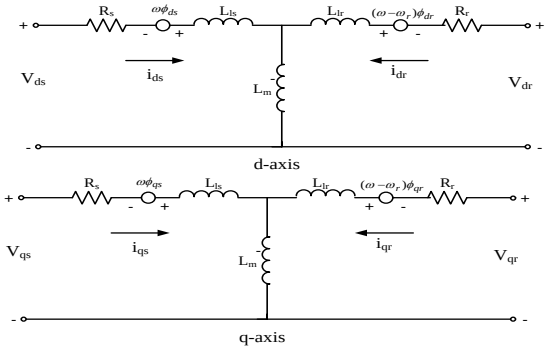

Fig. 3: The d-q equivalent circuit of DFIG [1].

2.2.2 Converter control system

The control system is an important issue for the wind turbine performance. It maximizes the extracted power from the wind and also makes sure that the delivered power to the grid complies with the interconnection requirements. A back to back converter is used to connect the generator to the grid and it allows the full controllability of the system. It comprises two parts: the rotor-side and the grid-side converters, with specific target for each one. The first one controls the speed, active power and reactive power, while the second one maintains the voltage on the DC-link at a constant value to transfer all generated power to the grid.

Rotor-side converter

The rotor-side converter converts the variable-frequency voltage into dc voltage. The rotor-side converter is used to control the active power of the DFIG and the voltage level measured at the stator terminals. It is important to control the DFIG output active power in order to adjust the angular speed of the turbine rotor so as to maximize the extracted power for a certain wind speed [12].

The current mode control is used to achieve the optimum wind power tracking [14]. The optimum mechanical power is defined according to the rotor speed. The reference reactive current, $I_{qr\text{-}ref}$, reflects the PI controller output, which depends on the error signal produced from comparing the actual and the required values of the reactive power. The rotor reference current has to be limited according the rotor-side converter rating. The reference components are compared with their actual components and the error signal is tuned through PI controller to represent the control contribution to correct the rotor voltage signal as illustrated in Fig. 4. The corrected rotor voltage waveform is introduced to the pulse width modulation (PWM) controller, as a reference waveform, to create the corresponding switching signals for the rotor-side converter.

Grid-side converter

The grid-side controller maintains the DC-link voltage at a certain desired value to transfer all power generated by rotor to the grid. As shown in Fig. 5, the control scheme consists of the following loops: The inner loops control the grid currents (current regulator loop) and the outer loops control the dc-link voltage (dc voltage regulator) and the reactive power (ac voltage regulator). The current regulator loop; that is responsible for controlling the magnitude and phase of the voltage generated by the PWM converter, i.e. V'_d and V'_q. This loop depends on I_{dref}, and $I_{qref,}$ reference currents produced respectively by the dc voltage and ac voltage regulators. The outer loops regulate the power flow of the system by controlling the active and reactive powers delivered to the grid. Further, unity power factor flow (zero reactive power exchange) could be easily obtained, unless the grid operators require different reactive power settings. The necessary measurements for the control system are ac voltages and currents at the grid side as well as the value of the dc voltage, while the ac-signals are transformed from the abc to their equivalents in the dq reference frame and thus offers much easier and more feasible controllability.

The DC link voltage can be expressed as [15]:

$$C\frac{dV_{dc}}{dt} = \frac{P_t - P_g}{V_{dc}} \qquad (3)$$

where: C is the DC link capacitance, P_t is the wind turbine power and P_g is the grid power.

3. PERFORMANCE ANALYSIS OF SCIG AND DFIG-BASED WIND TURBINE

To examine the performance of the SCIG and the implemented control schemes of DFIG based wind turbines, three cases studies considering different wind speed variations have been conducted.

3.1 Case (1) Step Change in Wind Speed Profile

A. Performance of SCIG-based wind turbine

It is assumed that the wind speed profile varies up and down as step function with mean wind speed 9 m/s, with a simulation time of 5 s, as illustrated in Fig. 6 (a). Fig.6 (b), describes the rotational speed of the generator, which varies with wind speed especially at sudden changes in wind speed profile, where the oscillation depends on the moment of inertia. As depicted in Fig.6 (c), the mechanical torque also changed with wind speed variation with negative values, indicating generation mode, and it is proportional to the cubic of wind speed. Fig.6 (d), shows the tip speed ratio, λ, varies with time and the wind turbine does not have the ability to maintain the tip speed ratio at its optimal value (λ_{opt} = 8.1) except at t = 1 s to 2.5 s, where the system operates at (V_{wind} = 9m/s). Consequently, the power coefficient C_p is different from the optimal value that provides the MPPT except the period (t=1 s to 2.5 s), where C_p = C_{p_max} = 0.48 as seen in Fig. 6 (e). Fig. 6 (f) shows that the power injected to the grid is dependent average wind speed. The reactive power fed from the grid is shown in Fig. 6 (g), which describes the reactive power absorbed by the generator.

B. Performance of DFIG-based wind turbine

Fig.7 (a) shows the wind speed profile varies up and down as step functions with average value of 9m/s with a simulation time of 5 s. Fig.7 (b) describes the rotational speed of generator which takes the same wind speed profile except at sudden change, where the moment of inertia appeared. When the wind speed increases, the input mechanical torque also increases as seen in Fig.7 (c). The torque takes negative value for generating power. The controller succeeded to adjust the rotational speed with wind speed variation to maintain tip speed ratio λ at optimum value λ_{opt}, which ensure maximum value of power coefficient $C_{p.}$ Consequently, MPPT is achieved as seen in Fig.7 (d) and Fig.7 (e) some notches appear at time 1 s and 2.5 s due to the sudden changes in wind speed.

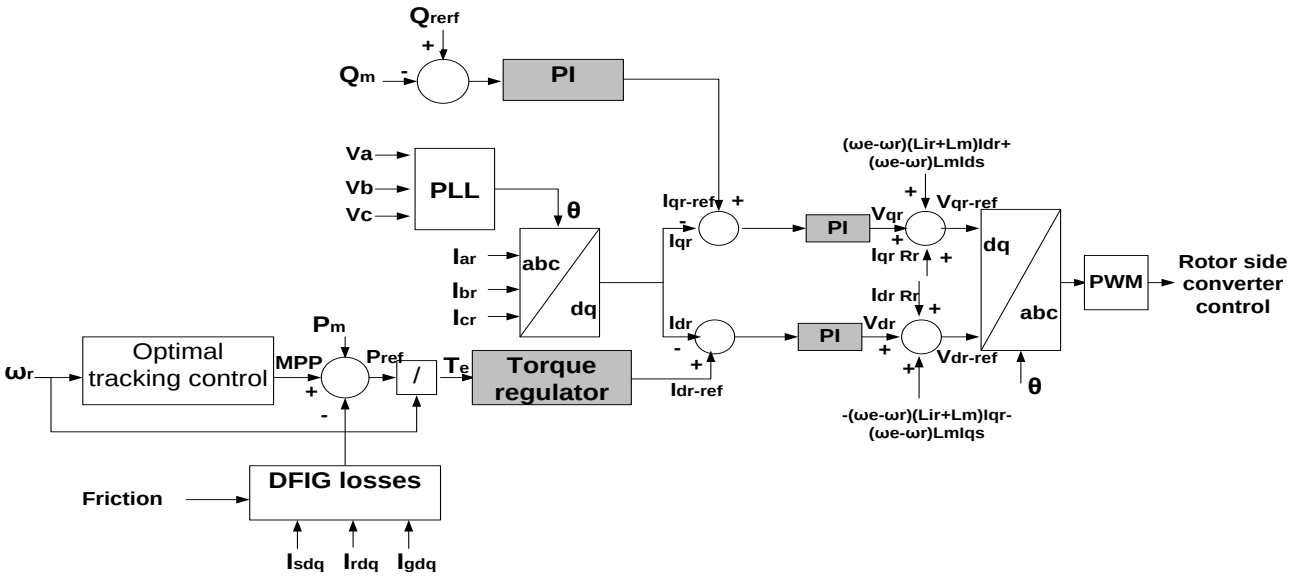

Fig. 4: Structure of control system for rotor-side converter [12].

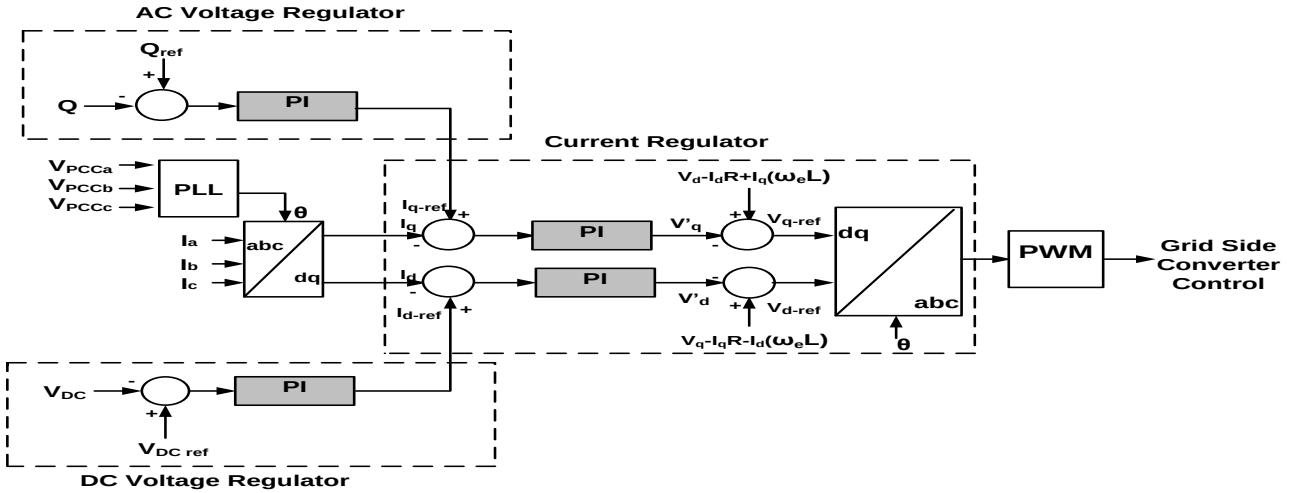

Fig. 5: Structure of control system for grid-side converter [1].

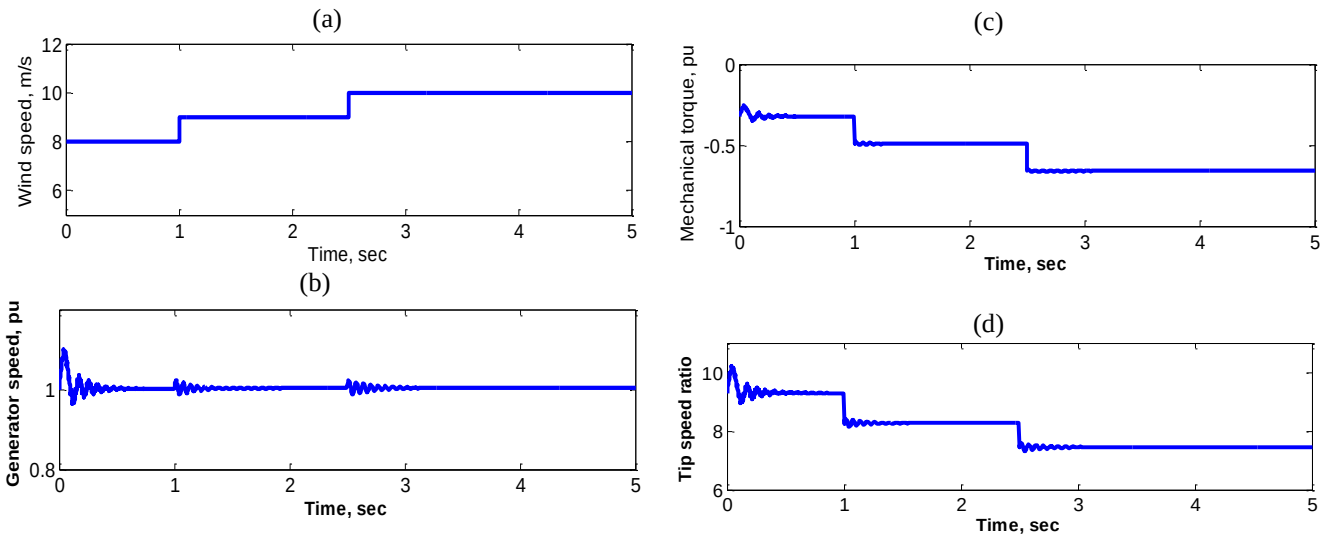

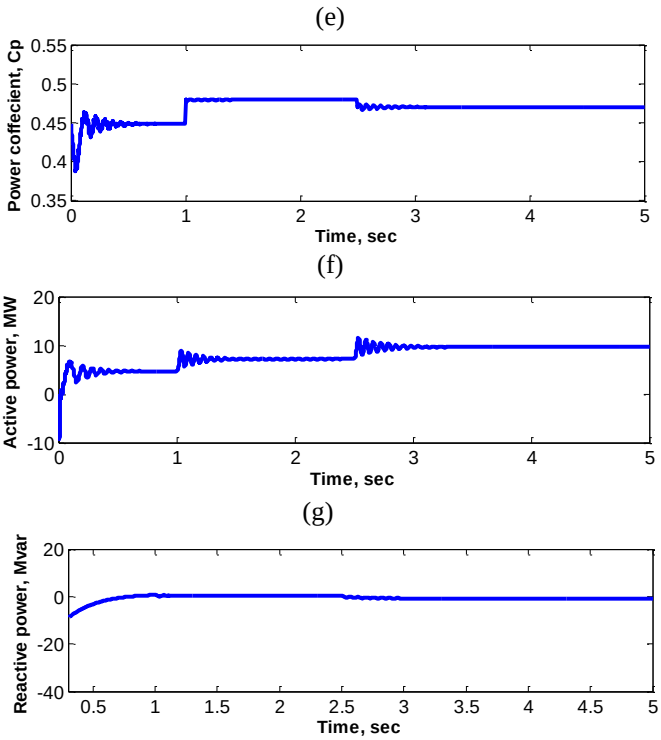

Fig.6: Constant speed system response for step changes in wind speed

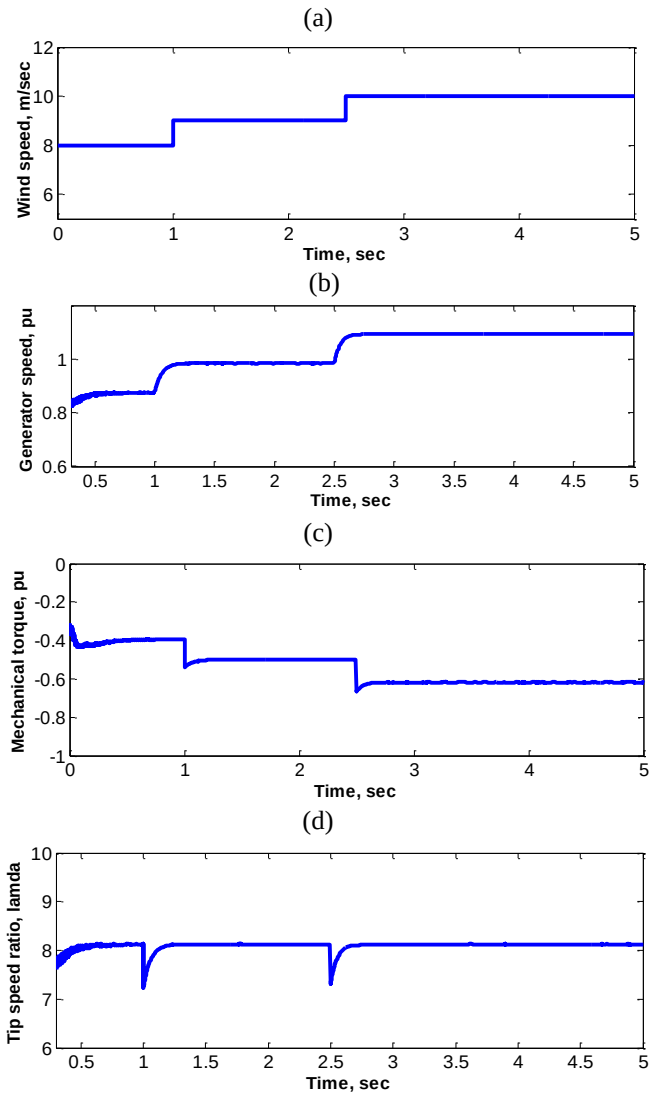

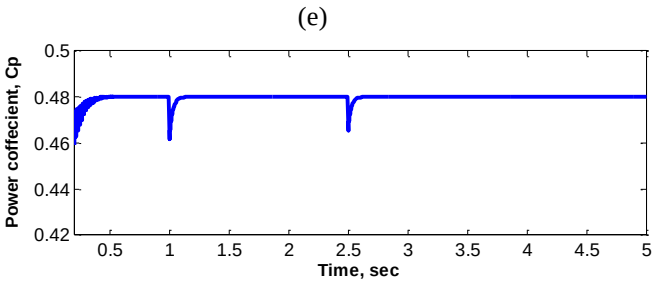

Fig.7: Rotor side converter response for step changes in wind speed

To realize the feasibility of the grid side converter controller, Fig.8 (a), Illustrate the dc link voltage. The controller gives good agreement between the actual and reference values of the dc link voltage, thus the controller capable to maintain dc voltage is almost constant at nominal value 1200 V except for at 1s, and 2.5s due to the sudden change in wind speed profile. Fig.8 (b) shows that the power injected to the grid is dependent on the average wind speed, the reactive power fed to the grid is shown in Fig.8 (c) which is approximately zero, i.e., the generator is working at unity power factor.

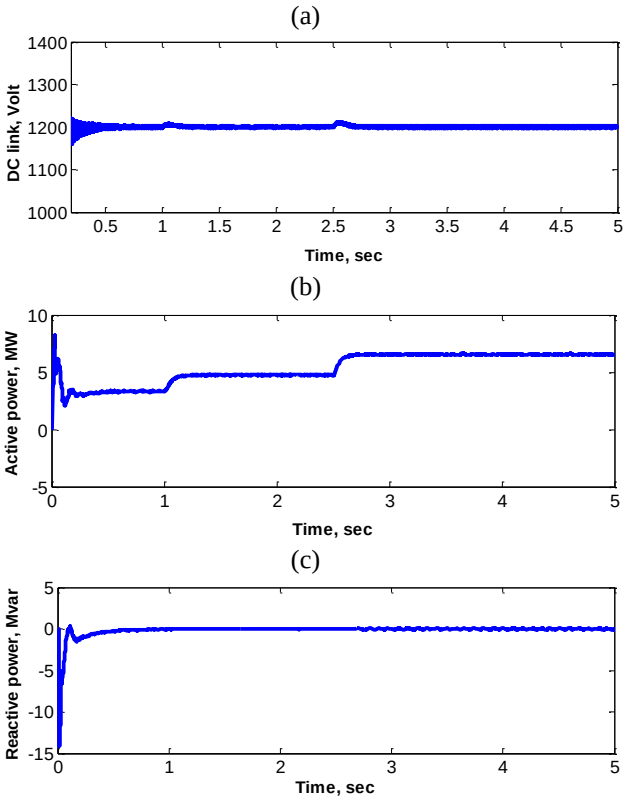

Fig.8: Grid side converter response for step changes in wind speed

3.2 Case (2) Ramp Change in Wind Speed Profile

A. Performance of SCIG-based wind turbine

Wind speed profile varies up and down with smooth ramp rates with average value of 9.5 m/s over a time span of 5 s as seen in Fig.9 (a). Fig.9 (b), and Fig.9 (c),

describe the rotational speed and the mechanical torque for the ramp wind speed, the generator rotational speed is almost constant with variation of wind speed. Fig.9 (d) and Fig.9 (e) demonstrate the tip speed ratio (λ) and power coefficient (C_p); it is obvious from these figures that λ and C_p are variation with time in constant speed wind turbine. Consequently, the maximum power tracking is not achieved.

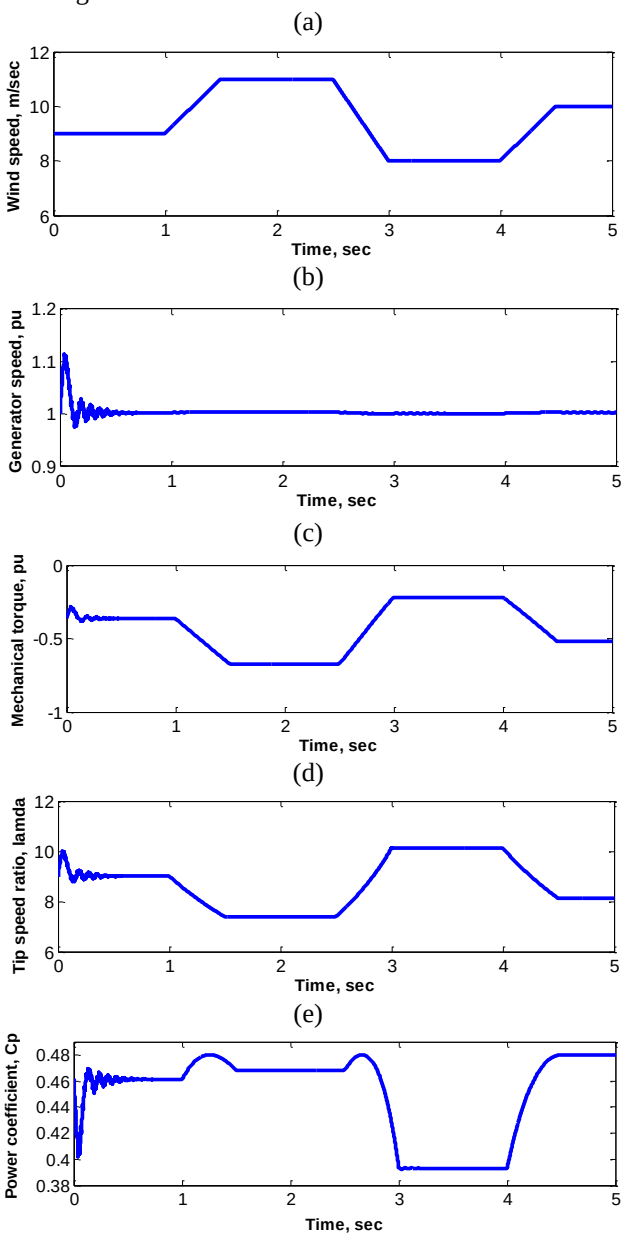

Fig.9: Constant speed System response for ramp changes in wind speed

B. Performance of DFIG-based wind turbine

It is assumed that the wind speed profile varies up and down with smooth ramp rates with a mean wind speed of 9.5 m/s as seen in Fig.10 (a) with a simulation time of 5 s. As shown in Fig.10 (b) the rotational speed of the generator various with wind speed profile. In addition, the mechanical torque is shown in Fig.10 (c) Moreover, the torque is negative, indicating input torque to the system, and it is proportional to cubic wind speed.

As shown in Fig.10 (d) and Fig.10 (e) respectively, the maximum power tracking is achieved and hence, the tip speed ratio λ is maintained at the corresponding optimal values and the power coefficient Cp is maintained constant at its maximum value.

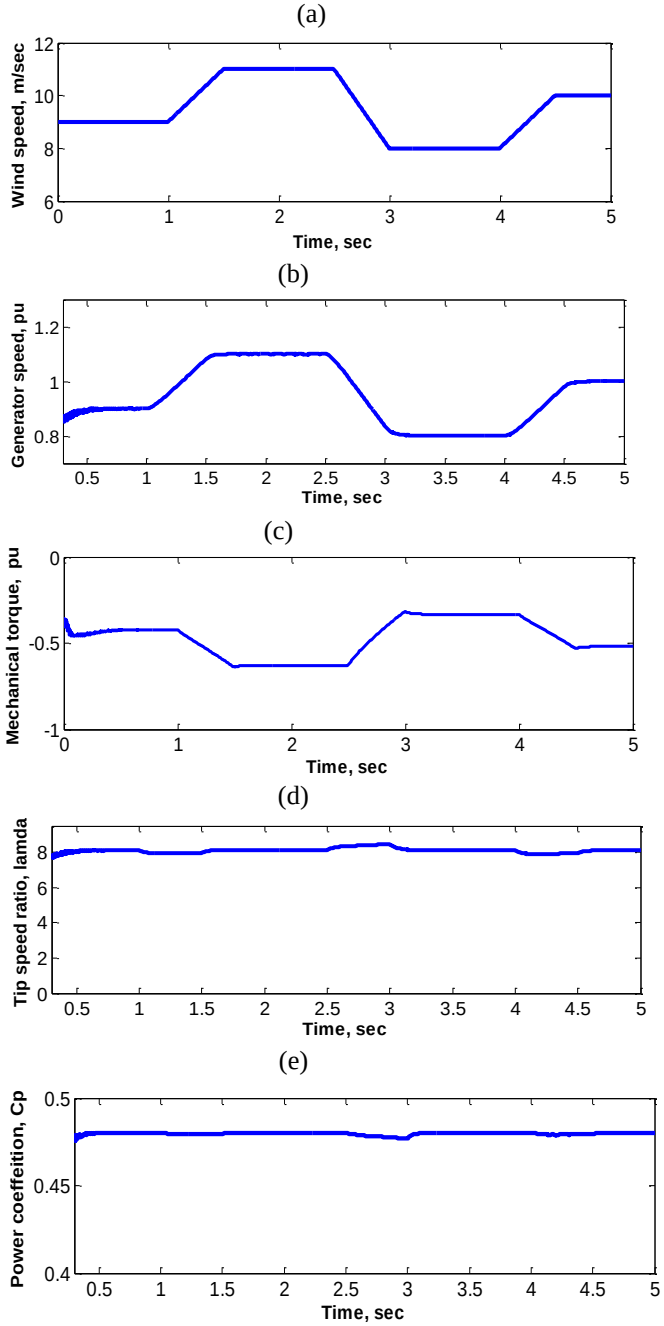

Fig.10: Variable speed System response for ramp changes in wind speed.

3.3 Case (3) Random Changes in Wind Speed Profile

A. Performance of SCIG-based wind turbine

In case (3), the wind speed, shown in Fig.11 (a), varies randomly with an average value of 10 m/s and 10% turbulence intensity. Wind speed time series is given according to the equivalent wind speed model provided

in wind turbine blockset, Matlab/Simulink [16]. Fig.11 (b) describes the rotation speed. The tip speed ratio (λ) and power coefficient (C_p) of wind turbine are given in Fig.11 (c), and Fig.11 (d), respectively. It is obvious from these figures that λ and C_p vary in the period conducted in simulation since no control is applied for wind turbine to achieve MPPT.

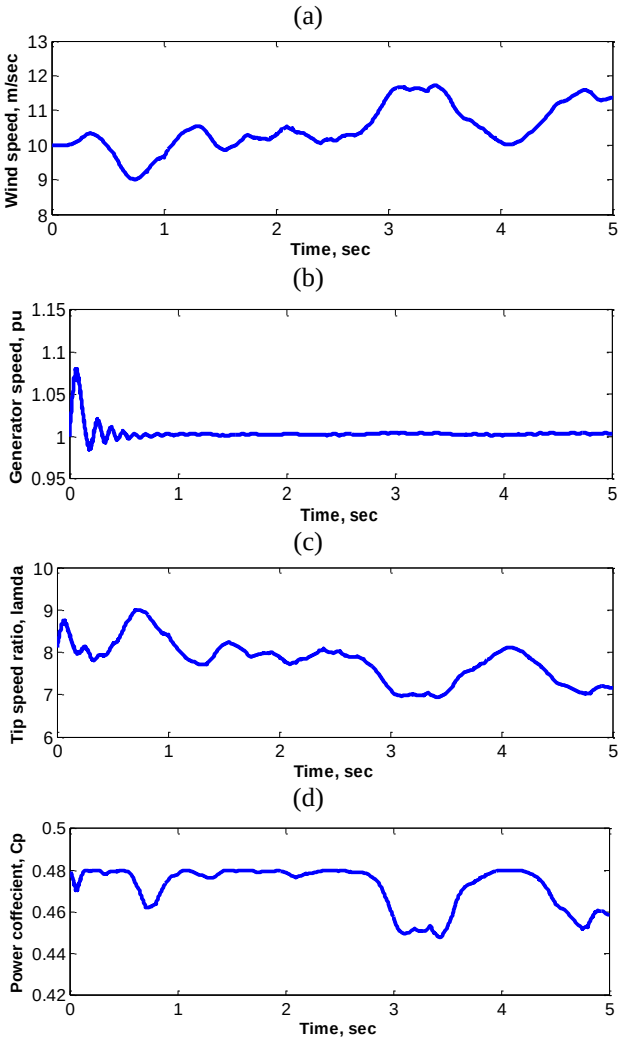

Fig.11: Constant speed System response for random changes in wind speed.

B. Performance of DFIG-based wind turbine

The wind speed profile, as seen in Fig.12 (a), varies randomly with an average value of 10 m/s and 12% turbulence intensity. The tip speed ratio and power coefficient of wind turbine are given in Fig.12 (b) and (c) respectively. It is obvious from these figures that λ_{opt} and C_{p_max} are almost constant for the period conducted in simulation. Similar to the previous cases, appropriate performance is obtained regarding to generator rotation speed with wind speed profile. These results are agreed with results in [15].

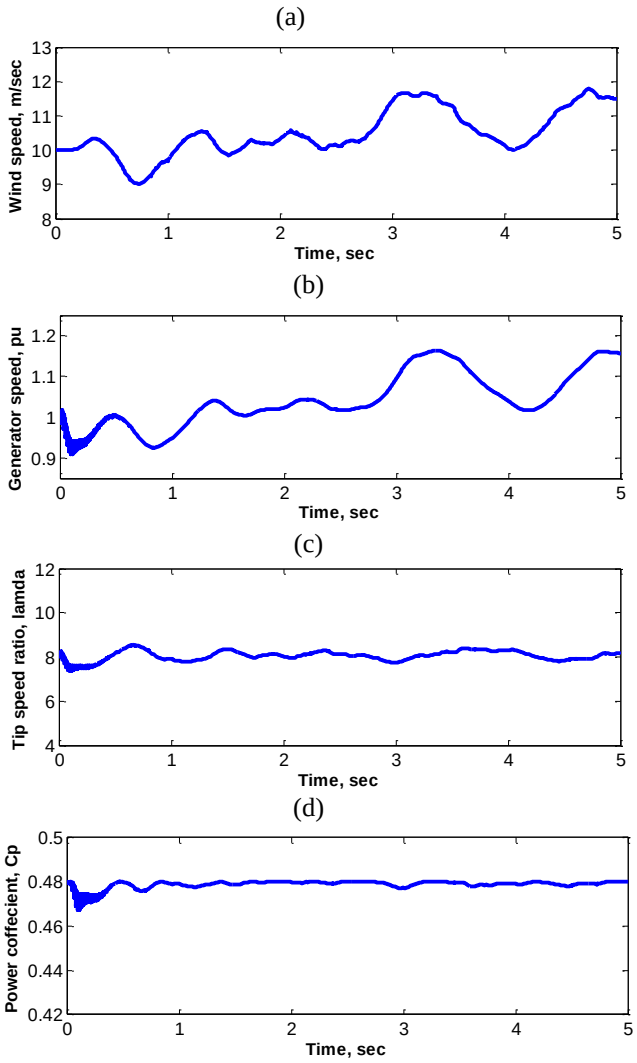

Fig.12: Variable speed System response for random changes in wind speed

4. FLICKER EMISSION OF INDUCTION GENERATOR-BASED GRID CONNECTED WIND TURBINES

A wind turbine with induction generator is integrated to external power system represented by constant voltage source connected in series with its Thevenin's equivalent impedance as shown in Fig. 13 (a). The phasor diagram is illustrated in Fig. 13 (b).

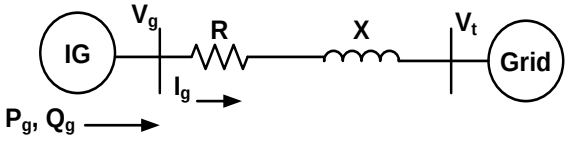

(a)

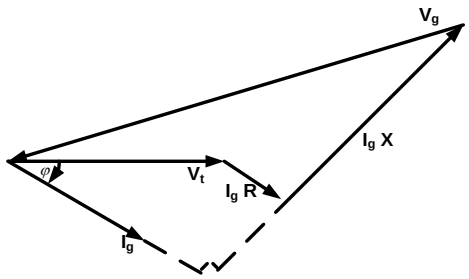

(b)

Fig.13 (a) A simple diagram for IG-based wind turbine connected to grid, and (b) phasor diagram.

The active and reactive power exchange at PCC is varying according to the incident wind speed and; as a result, the voltage at this point will fluctuate. From Fig. 13, the voltage difference between the generator and grid can be approximated as follows:

$$V_g - V_t = \Delta V = I_g^*(R + jX) = (\frac{P_g - jQ_g}{V_g})(R + jX) \quad (4)$$

$$\Delta V = \frac{P_g.R + Q_g.X}{V_g} + j\frac{P_g.X - Q_g.R}{V_g} \quad (5)$$

If it is assumed that the imaginary component in (5) is negligibly small compared to the real component, then the voltage difference is simplified to:

$$\Delta V = \frac{P_g.R + Q_g.X}{V_g} \quad (6)$$

Consequently; if the variation of the active power injected to the grid is ΔP and the corresponding variation of the reactive power delivered to the grid is ΔQ, then voltage fluctuation, at PCC, ΔV, is given as follows:

$$\Delta V = \frac{\Delta P_g.R + \Delta Q_g.X}{V_g} \quad (7)$$

This can be rewritten as follows;

$$\Delta V = \frac{\Delta S.Z.\cos(\theta + \varphi)}{V_g} \quad (8)$$

where R is the resistance of the grid impedance (pu), X is the reactance of the grid impedance (pu), ΔS is the apparent power variation, $\Delta S = \sqrt{\Delta P^2 + \Delta Q^2}$ (pu), Z is the grid impedance amplitude (pu), θ is the grid impedance angle, $\theta = \tan^{-1}(\frac{X}{R})$, and φ is $\tan^{-1}(\Delta Q/\Delta P)$.

From (7), it is obvious that the voltage fluctuation is not only dependent on the reactive power variation, ΔQ, but also on the active power variation ΔP. Voltage flicker is typically assessed by a standard flickermeter. The nominal voltage is assumed to be 1.0 pu.

5. FLICKERMETER MODEL

Flicker, which is one of the important power quality aspects, is defined as *"An impression of unsteadiness of visual sensation induced by a light stimulus, whose luminance or spectral distribution fluctuates with time"* [17]. Flicker level is measured by the use of a flickermeter described in IEC 61000-4-15. The flicker level depends on the amplitude, shape and repetition frequency of voltage fluctuation. The flickermeter, shown in Fig. 14, takes voltage as an input and gives the short-term flicker index, P_{st}, as an output. The flickermeter comprises two main parts: 1) A simulator for the response of the lamp–eye–brain chain. 2) An on-line statistical analyzer of the flicker signal and a demonstrator of the results [18].

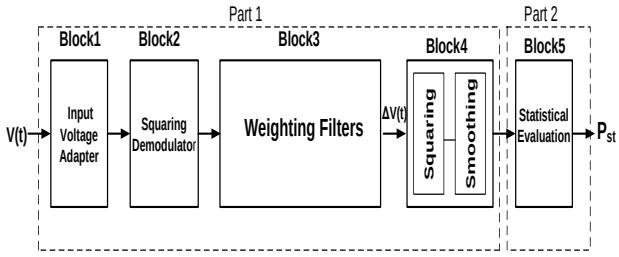

Fig. 14: Block diagram of flickermeter according to IEC 61000-4-15 [18].

6. SIMULATION RESULTS AND DISCUSSION FOR FLICKER MODELING

Owing to the characteristics of directly-connected constant-speed wind turbines and the variable speed DFIG-based wind turbines, the active and reactive power exchange at the PCC varies according to the incident wind speed. As a result, the voltage at this point will fluctuate. Voltage fluctuation caused by these wind turbines raises certain limitation regarding the penetration level of the wind generation since it can result in serious electrical disturbances to the grid. Consequently, the use of STATCOM to minimize the voltage fluctuation for constant speed wind turbines is essential. The impacts of different factors on the short-term flicker index, P_{st}, are presented in the following subsections.

6.1 The effect of short circuit ratio (SCR)

As a comparative between DFIG and SCIG in Table 1 and Fig. 15 shows the effect of SCR on the short-term flicker index P_{st}. This simulation is carried out, where the mean wind speed at hub level is maintained at 10 m/s, the site turbulence is 12% and the X/R ratio equal to 10. From table 1 and Fig. 15, it can be seen that the flicker level decreases with the increase of short circuit ratio. In addition, the effect of the STATCOM is highly significant in weak grids; however, the STATCOM effect becomes weaker with stiff grids. Also, the variable speed DFIG-based wind turbines have shown better

performance regarding voltage fluctuation compared to constant speed SCIG-based wind turbines for all values of SCR. The reason is that variable-speed operation of the rotor has the advantage that the sharp power variations are not transmitted to the grid due to the presence of interfacing converters. These results are agreed with results in [10].

Table 1: The effect of SCR on the $P_{st.}$

SCR (pu)	P_{st} at SCIG	P_{st} at SCIG with STATCOM	P_{st} at DFIG
10	2.3812	1.2160	1.0803
20	1.2422	0.8663	0.6362
30	0.8937	0.7539	0.5969
40	0.7448	0.6733	0.5701
50	0.6747	0.6323	0.5611

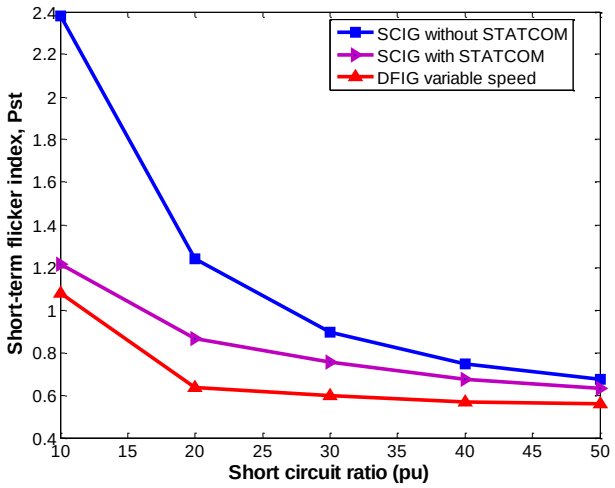

Fig. 15: The effect of SCR on the short-term flicker index $P_{st.}$

6.2 The effect of grid impedance angle

As a comparative between DFIG and SCIG in Table 2 and Fig. 16 show the variation of the flicker emission with the impedance angle θ, ($\theta=\tan^{-1}(X/R)$). The SCR is maintained at 50 pu. The mean wind speed at hub level is 10 m/s and site turbulence is 12%. From table 2 and Fig. 16, it can be seen for constant speed operation that the flicker decreases with increase of θ to a certain minimum point and, then, the flicker increases again with increase of θ. The minimum point here is recognized at $\theta \approx 45°$ at SCIG. In addition, the STATCOM reduces the flicker emission of constant-speed wind turbines. The effect of the STATCOM is significant when the grid impedance is highly inductive as illustrated in Fig. 16. On the other hand, the voltage flicker effect on DFIG is lower than the effect on SCIG, where the P_{st} is almost constant at very low levels as shown in table 2 and Fig. 16.

Table 2: Variation of P_{st} with the grid impedance angles.

ϴ =$\tan^{-1}$(X/R)	$P_{st,}$ at SCIG	$P_{st,}$ at SCIG with STATCOM	P_{st} at DFIG
0	0.6970	0.6954	0.5610
5	0.6706	0.6682	0.5600
15	0.6191	0.6149	0.5570
25	0.5855	0.5795	0.5560
35	0.5643	0.5613	0.5561
45	0.5594	0.5571	0.5550
55	0.5712	0.5622	0.5549
65	0.5970	0.5702	0.5547
75	0.6337	0.5882	0.5543
85	0.6775	0.5920	0.5540
89.995	0.6974	0.6570	0.5553

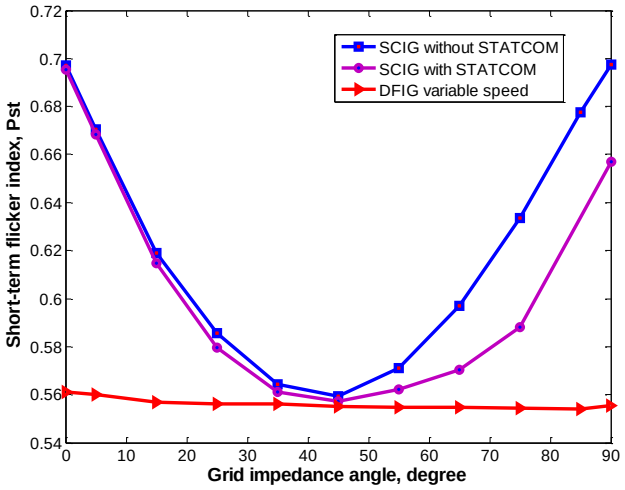

Fig. 16: Variation of $P_{st}$with the grid impedance angle

6.3 The effect of mean wind speed at hub level

As a comparative between DFIG and SCIG in Table 3 and Fig. 17 show the effect of mean wind speed on the short-term flicker index, P_{st} at X/R ratio equal to one and turbulence intensity equal to 12%. The flicker emission increases with increasing wind speed. Saturation or flat variation is recognized when the mean wind speed exceeds the rated value. The flicker emission effect on DFIG increases slightly with the increase of the mean wind speed and the effect of the STATCOM is significant when the grid impedance is highly inductive (high X/R ratio). Consequently, the DFIG shows better performance than SCIG as shown in table 3 and Fig.17.

Table 3: Variation of P_{st} with the mean wind speed

Mean wind speed (m/s)	P_{st}, at SCIG	P_{st}, at SCIG with STATCOM	P_{st} at DFIG
10	0.6747	0.5812	0.5611
12	0.7194	0.6280	0.5632
14	0.7477	0.5990	0.5607
16	0.7541	0.6128	0.5612
18	0.7576	0.6342	0.5624

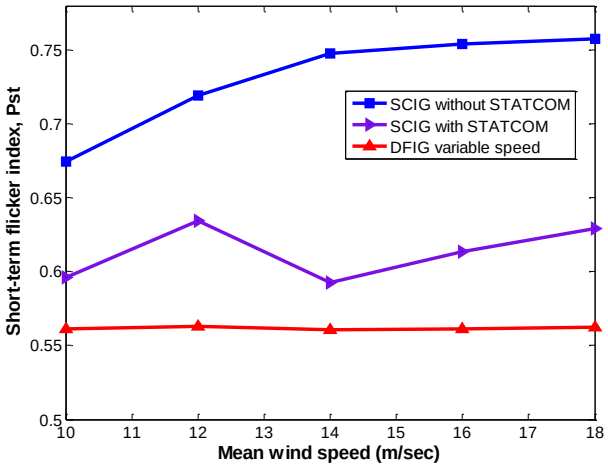

Fig. 17: Variation of P_{st} with the mean wind speed

6.4 The effect of turbulence intensity

In this case, the mean wind speed at the hub level is maintained at 10 m/s, the fault current level is 10 pu, and the grid impedance angle is 45°.Table 4 and Fig. 18, show the variation of P_{st} with the turbulence intensity. The increase in the wind speed turbulence increases the power variability and thus, the flicker emission increases with the increase of the turbulence intensity. The effect of the STATCOM is significant with weak grids. From the table 4 and Fig. 18, the short-term flicker index, P_{st}, value for DFIG less than short-term flicker index, P_{st}, value for SCIG. Consequently; DFIG is better than SCIG regarding the flicker emission with the increase of the turbulence intensity.

Table 4: Variation of Pst with wind speed turbulence.

Turbulence intensity	P_{st}, at SCIG	P_{st}, at SCIG with STATCOM	P_{st} at DFIG
5%	2.6669	1.2979	0.801
10%	2.6722	1.3565	0.820
15%	2.6775	1.3612	0.8910
20%	2.6827	1.4559	0.930
25%	2.6879	1.3242	1.170

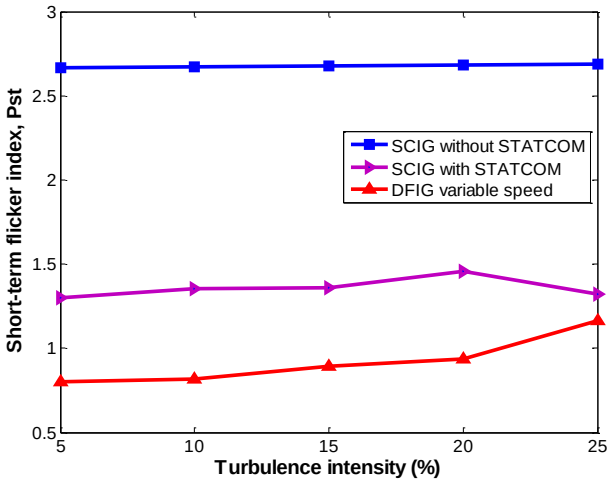

Fig.18: Variation of P_{st} with wind speed turbulence.

7. CONCLUSION

This paper presented a comparative performance analysis and flicker emission of SCIG and DFIG based wind turbines. From simulation results the variable speed DFIG based wind turbines give better performance than constant speed SCIG based wind turbines under different wind speed conditions and to achieve maximum power point tracking (MPPT) due to the control flexibility. Based on the developed wind turbine model, the flicker emission of constant speed wind turbines with SCIG and variable speed wind turbines with DFIG are investigated. Simulation results show the flicker level increases with increasing in turbulence intensity and mean wind speed however, it decreases with the increase of the grid impedance angle and short circuit ratio. The STATCOM has showed significant effect when the grid impedance is highly inductive (high X/R ratio). Although the risk of flicker emission for resistive grids (low X/R ratio) is increased, the STATCOM effect becomes weaker than its effect for inductive grids. Generally, variable-speed wind turbines have shown better performance regarding the flicker emission compared to constant-speed wind turbines.

REFERENCES

[1] W. S. E. Abdel-Latif, A. H. K. Alaboudy, H. E. Mostafa and M. Y. Fekry, " Evaluation and mitigation of voltage flicker caused by constant speed wind turbines," IEEE PES ISGT Middle East Conference, Saudi Arabia, Dec. 2011.

[2] T. Ackermann, "Wind power in power systems," book, John Willey and Sons, 2005.

[3] S. Vitanova, V. Stoilkov and V. Dimcev, "Comparing SCIG and DFIG for wind generating conditions in Macedonia" International Conference on Renewable Energies and Power Quality (ICREPQ'11), Las Palmas de Gran Canaria (Spain), 13-15 April, 2011.

[4] M. Anju, and R. Rajasekaran, "Power system stability enhancement and improvement of LVRT capability of a DFIG based wind power system by using SMES and SFCL" *International Journal of Electrical and Computer Engineering (IJECE)*vol. 3, no. 5, October 2013, pp. 618~628.

[5] B. Gandhi, K. K. Mohiuddin, and T.V.V P. Kumar "Enhancement and improvement of wind power system by using SMES and SFCL" *International Journal of Computer Science and Mobile Computing*, vol.3, issue.10, pp. 387-392, Oct. 2014.

[6] A. Awasthi, R. Diwan and M. Awasthi,"Study for Performance Comparison of SFIG and DFIG Based Wind Turbines" *International Journal of Latest Trends in Engineering and Technology (IJLTET)*, vol. 2 Issue 4, July 2013.

[7] M. Machmoum, A. Hatoum, T. Bouaouiche, "Flicker mitigation in a doubly fed induction generator wind turbine system," Math. Comput. Simul, 2010.

[8] Å. Larsson, "Flicker emission of wind turbines during continuous operation," *IEEE Trans. Energy Conversion*, vol. 17, no. 1, pp. 114-118, Mar. 2002.

[9] C.Carrillo, E.Diaz-Dorado, and J.Cidras "PSCAD/EMTDC- based modling and flicker estimation for wind turbines" Europe Premier Wind Energy Event. EWEC, Marseille. 2009.

[10] Z. Chen, J. M. Guerrero, and F. Blaabjerg, "A review of the state of the art of power electronics for wind turbines" *IEEE Trans. Energy Conversion*, vol. 24, no.8, Aug. 2009.

[11] M. E. Elshiekh, D. A. Mansour,,andA. M.Azmy "Improving fault ride-through capability of DFIG-based wind turbine using superconducting fault current limiter" *IEEE Trans. on Applied Superconductivity*, vol. 23, no. 3, June 2013.

[12] Walid S. E. Abdellatif , Ali H. Kasem Alaboudy ,and Ahmed M. Azmy" Evaluation of voltage flicker emissions of variable speed DFIG-based wind turbines" 3rd International Conference on Energy Systems and Technologies, , Cairo, Egypt, 16 – 19 Feb. 2015.

[13] H. Sang Ko, G. Yoon, N. H. Kyung and W. P. Hong "Modeling and control of DFIG-based variable-speed wind-turbine" *Electric Power Systems Research*, no. 78, pp. 1841–1849, 2008.

[14] H. Li, and Z. Chen, "Overview of different wind generator systems and their comparisons," *IET Renew. Power Geneerators*, vol. 2, no. 2, pp. 123–138, 2008.

[15] A. H. K. Alaboudy, A. A. Daoud, S. S. Desouky, and A. A. Salem**,** "Converter controls and flicker study of PMSG-based grid connected wind turbines", *Ain Shams Engineering Journal, Elsiever*, vol. 4, issue 1, pp. 75-91, Mar. 2013.

[16] F .Iov, A. D. Hansen, P. Sorensen, and F.Blaabjerg. "Wind turbine blackest in Matlab/Simulink," Research Project, Institute of Energy Technology, Alborg University, Mar. 2004.

[17] Y. Kim, A. Marathe and D. Won " Comparison of various methods to mitigate the flicker level of DFIG in considering the effect of grid conditions" *Journal of Power Electronics*, Vol. 9, No. 4, July 2009.

[18] IEC61000-4-15: 'Electromagnetic compatibility (EMC). Part 4: testing and measurements techniques – Section 15: flickermeter, functional and design specifications' (1997, 1st edition).